

LA-UR -81-2303

CONFIDENTIAL - 9/1

**TITLE:** SOME TECHNIQUES AND RESULTS FROM HIGH-PRESSURE SHOCK-WAVE  
EXPERIMENTS UTILIZING THE RADIATION FROM SHOCKED TRANSPARENT MATERIALS

**AUTHOR(S):** R. G. McQueen and J. N. Fritz

**MASTER**

**SUBMITTED TO:** AIP 1981 Conference on Shock Waves in Condensed Matter  
Palo Alto, CA, June 1981

University of California

By acceptance of this article, the publisher recognizes that the U.S. Government retains a nonexclusive, royalty-free license to publish or reproduce the published form of this contribution, or to allow others to do so, for U.S. Government purposes.

The Los Alamos Scientific Laboratory requests that the publisher identify this article as work performed under the auspices of the U.S. Department of Energy.



**LOS ALAMOS SCIENTIFIC LABORATORY**

Post Office Box 1663 Los Alamos, New Mexico 87545

An Affirmative Action/Equal Opportunity Employer

REPRODUCTION OF THIS DOCUMENT IS UNLIMITED

# SOME TECHNIQUES AND RESULTS FROM HIGH-PRESSURE SHOCK-WAVE EXPERIMENTS UTILIZING THE RADIATION FROM SHOCKED TRANSPARENT MATERIALS

R. G. McQueen and J. N. Fritz  
Los Alamos National Laboratory

## ABSTRACT

It has been known for many years that some transparent materials emit radiation when shocked to high pressures. We have used this property to determine the temperature of shocked fused and crystal quartz, which in turn allowed us to calculate the thermal expansion of  $\text{SiO}_2$  at high pressure and also the specific heat. Once the radiative energy as a function of pressure is known for one material we show how this can be used to determine the temperature of other transparent materials. By the nature of the experiments very accurate shock velocities can be measured and hence high quality equation of state data obtained. Some techniques and results are presented on measuring sound velocities from symmetrical impact of nontransparent materials using radiation emitting transparent analyzers, and on nonsymmetrical impact experiments on transparent materials. Because of special requirements in the later experiments, techniques were developed that lead to very high-precision shock-wave data. Preliminary results, using these techniques are presented for making estimates of the melting region and the yield strength of some metals under strong shock conditions.

## INTRODUCTION

Los Alamos has been using the radiation from shocked gases for many years to obtain equation of state data for other materials by the flash gap technique developed by J. M. Walsh.<sup>1</sup> Most of those experiments were performed on materials where no radiation could be expected to be observed, and the few where it might be were usually shielded by shims. Probably the first to utilize the radiation emanating from the shock front in materials pertinent to this report was the work of Kormer et al.<sup>2</sup> reported in 1965. They used this effect to infer the temperature of some shocked solids. Until the last few years this powerful tool was not exploited.

During the following years considerable effort was made to measure the sound velocity at high pressures; by ourselves and others, Al'tshuler et al.<sup>3</sup> in particular. Such efforts, if successful, could yield the longitudinal and bulk sound velocities and hence the shear moduli and the quest of the last decade or so; the elusive Grüneisen parameter. These early measurements were basically of the x-t type and hence not time resolved. The early time resolved measurements were limited to low pressure experiments. The ASM probe<sup>4</sup> and VISAR<sup>5</sup> opened a new range of high pressure time resolved experimentation.

The techniques described here were developed for two reasons: one to measure the radiation temperature of shocked transparent materials; and two to measure the location of overtaking rarefaction waves behind strong shocks and hence determine the

velocity of sound waves at high pressure. In addition observation of the radiation from the shock wave has led to the development of several very accurate shock velocity measuring systems.

In 1968 we performed several experiments to determine the overtaking wave velocity in fused quartz impacted by a stainless steel driver plate. The fused quartz target assembly consisted of a stack of plates held together by double stick tape so that a small  $\sim .05$  mm gap separated the plates in the central region. This area was viewed through a small slit with a sweeping image camera. It was felt then, and now, that by observing the shock arrival at the various gaps through the same slit that the shock velocities could be measured very accurately through each layer. These records clearly show the shock arrival at the various levels. In Fig. 1-a the calculated shock velocity vs thickness shows pretty much where the rarefaction overtakes the shock, but clearly more or higher quality data would be needed to locate accurately the exact overtake position. Undoubtedly the most important feature of these records was ignored; that of the intense film darkening at the beginning of the record and subsequent decrease. This record shows that fused quartz radiates copiously and that this could be used to determine its temperature. Moreover it showed that these measurements offer a sensitive method of determining overtake wave velocities. It was over ten years later, while we were now in our present endeavors that these old experiments were recalled. A microdensitometer scan was made of one of the records and plotted 1-b. This shows the radiation from the flash gaps as well as the decrease caused by the pressure

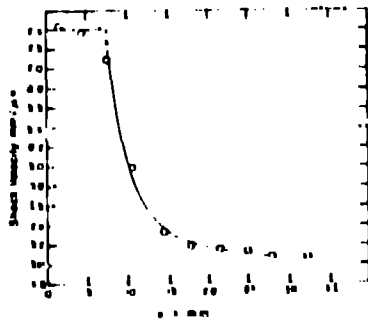


Fig. 1-a. Shock velocity vs thickness through a stack of fused quartz plates.

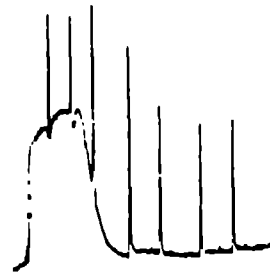


Fig. 1-b. Microdensitometer scan of the photographic record. The spikes are from the flash gaps.

release due to the flash gaps. The most salient feature of course is the decrease in radiation caused by the overtaking release wave. The electronic equipment to exploit these phenomena were available at the time. For example we are using photomultipliers developed even earlier. This should have been a most shining example of serendipity but unfortunately we were looking in a different direction. It is also of interest that the decrease in radiation due to the rarefaction overtake seen by Kormer et al.<sup>2</sup> was also disregarded as an experimental technique.

High quality shock velocity measurements can be made by monitoring changes in radiation levels as the shock passes various interfaces. Since these interfaces can be made to have negligible

thickness one has in effect zero-perturbation time markers. The application for making shock velocity measurements will be noted where appropriate since they are usually required as part of either the temperature or overtake measurement.

### RADIATION TEMPERATURE MEASUREMENTS

There are several ways to obtain temperatures from radiation measurements. The distinction is basically the difference from looking at the radiation from the following sources: narrow band widths centered on a few wave lengths, so called color temperatures; many small discrete intervals, spectral analysis,<sup>6</sup> and over a broad spectral range, the brightness temperature. We have used brightness temperatures here primarily because of the work done by W. Davis of this laboratory. He determined the brightness temperature of detonating nitromethane by photographic techniques. Since we have comparable photographic capabilities here, we decided to use his work to calibrate the relative radiation of shocked materials to detonating nitromethane.

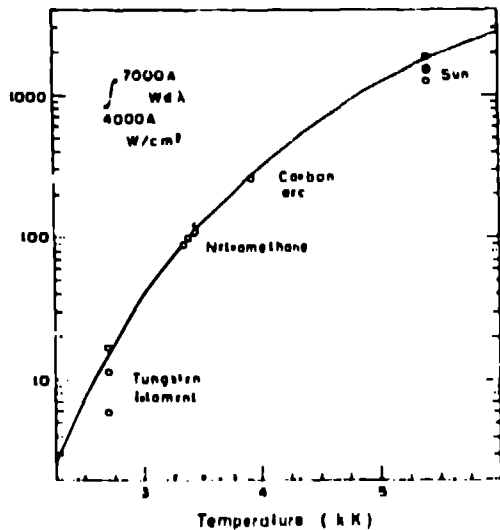


Fig. 2. W. Davis's nitromethane calibration function.

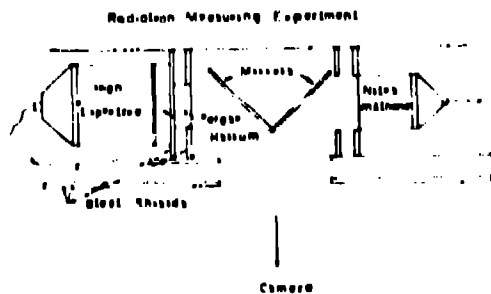


Fig. 3. High explosive system to view both the nitromethane standard and the unknown.

To establish his standards he calibrated to a tungsten filament, the carbon arc and the sun. Assuming that the photographic film responds uniformly to the radiation between 400 and 700 nm he calculated the curve (Fig. 2) of the energy radiated as a function of temperature. The calibration points are plotted on this curve at their estimated temperature with their converted measured brightness to the radiated energy scale, along with the measured nitromethane points. In these experiments we compare the relative intensity of shocked quartz to that of detonating nitromethane by viewing each through discrete openings of various widths placed on the cover plate. The same plate with a range of four in widths was used for many of the nitromethane standards. A suite of cover plates; usually four steps with a range of two were used for the unknown. By suitable combinations over two orders of magnitude in intensities could be compared. An explosive system used on some experiments (as shown in Fig. 3) and a reproduction of a photographic record in Fig. 4. A microdensitometer scan of the record is reproduced in Fig. 5.

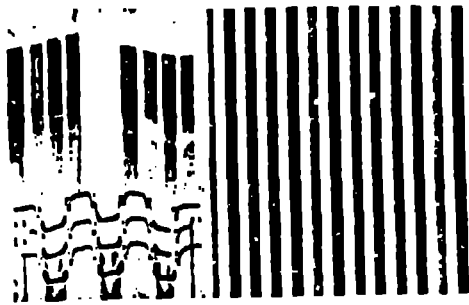


Fig. 4. Photographic record. The unknowns are on the left. The bands on the right are the standards.

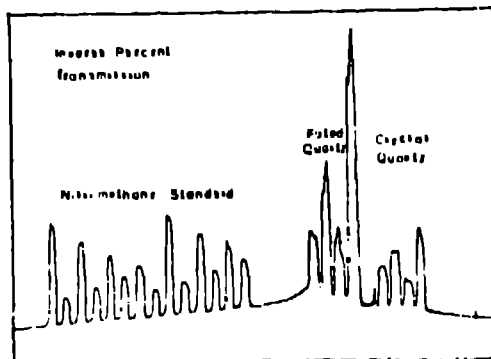


Fig. 5. microdensitometer scan of a photographic record.

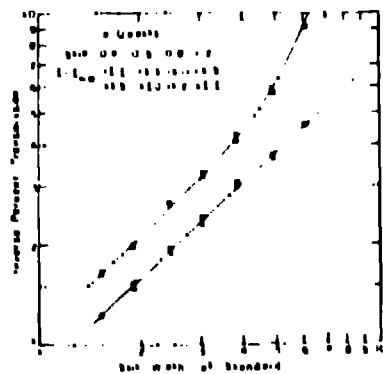


Fig. 6. Inverse percent transmission vs slit width on the nitromethane.

Both film densities and inverse percent transmission of the records have been used to determine relative intensities. A plot of inverse percent transmission of the standard (Fig. 6) gives an indication of the inherent precision of these measurements. The o's and x's are readings from openings of the same width but different location. The two curves on the plot are readings obtained from different settings of the controls of the microdensitometer. Comparing the measured values of the quartz with these curves gives the relative intensities of the unknown to nitromethane.

The results of these measurements are given in Fig. 7 where we have plotted the relative intensities for both fused and crystal quartz as a function of shock particle velocity or what is equivalent to the square root of the internal energy. Below 4.0 km/s both fused and crystal quartz lie on the same curve and except for the region around 4.2 km/s, are approximately on the same but different curve in the higher pressure regime. Clearly in the region from 4.0-4.2 km/s a phase change has occurred. This was first reported at the fall AGU Meeting in 1979. In fused quartz shocked above 4.2 km/s the photographic records show that as the rarefaction from the HE side of the driver overtakes the shock in the quartz that there is first a decrease in radiation and then an increase which on occasion rises to higher levels than the original radiation. This can be seen in 8-a where a reproduction of an oscilloscope record shows the time

history of fused quartz shocked to a particle velocity of approximately 4.2 km/s. There is a fairly rapid increase in radiation, ~ 10 ns, followed by a near constant level and then an increase and subsequent decrease. Examination of the region just before the increase shows a slight decrease. What has happened is that the rarefaction has just overtaken the shock front and with

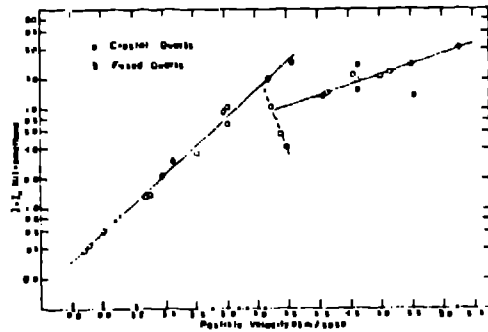


Fig. 7. Internal energy vs relative radiation energy for  $\text{SiO}_2$ .

the intensity is greater than the maximum of the low pressure fused quartz data. This is not an indication of an error since at a given particle velocity the pressure will be considerably higher. This effect can be seen in Fig. 8-b where crystal quartz (with a piece of fused quartz placed on it) was impacted into this pressure regime. The decrease in intensity is due to the shock entering the high pressure phase of the fused quartz. The rarefaction eventually catches the shock and the pressure decreases until it reaches the phase line where the radiation behaves as in 8-a. We also note that the four high pressure crystal quartz points show a lot of scatter. These four points actually are from only two shots. It appears that in this pressure regime the quartz has an initial level of radiation that falls off fairly rapidly to a lower but constant level. An oscilloscope record showing this is reproduced in Fig. 8-c.

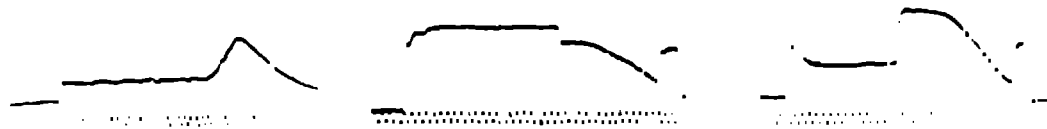


Fig. 8. Oscilloscope records. (a) Shock running through fused quartz showing the increase in radiation just as the shock wave is degraded by the rarefaction wave. (b) Shock into crystal quartz below the phase change showing sharp decrease in intensity when it reaches fused quartz. Fused quartz is shocked into the high pressure phase. The rarefaction in the fused quartz shows the same features as 8-a. (c) Relaxation seen in other experiments. The radiation increases when it enters the fused quartz. Rarefaction behavior is the same but modified because of the higher pressure.

This would appear to be a manifestation of a metastable state relaxing to some equilibrium value. There are still some interesting features of the behavior of shocked  $\text{SiO}_2$  that additional experiments might resolve. In particular are the oscillations in fused quartz when shocked directly into the transition region. This phenomena was reported in the 1979 AGU Meeting. We have since observed this four times, twice with photomultiplier systems. The data of Fig. 7 have been transformed to temperature vs pressure via Fig. 2. We have used those P-T curves to determine the specific heat at constant volume and the thermal expansion at constant pressure. In this work

reciprocity of the film response was tested and found to be good over a couple orders of magnitude as well as the black body assumption.

#### RADIATION MEASUREMENTS USING OTHER DETECTORS

Probably the most desirable feature of the measuring technique just described is having a calibrated standard on each experiment. In addition the logarithmic response of the film, while losing sensitivity, makes it almost impossible not to obtain some data on an experiment. The disadvantages are problems associated with scattered light, nonuniform background and the loss of sensitivity just mentioned. It is well known that photodiodes and photomultipliers have a linear response to radiation over a fairly large range of intensity. This makes them logical choices for measuring radiation temperatures. One weakness in using these is that the system must be calibrated, usually with a tungsten filament. While we have a black body furnace that can be used to almost 3000 K, the most difficult problem is calibrating the system so that the static and dynamic outputs are exactly the same. Accounting for window surfaces is nontrivial and putting a detonating nitromethane radiation pulse on the records through the same optical system is probably impossible. What we have done is something very close to the impedance match technique developed by Walsh.<sup>7</sup> In fact for complete analysis of the experiment one must make such a calculation. We simply sandwich the material to be investigated between two pieces of a "standard." The standard should be characterized both hydrodynamically, so the impedance match calculation can be made, and radiatively wise so that the radiation from the unknown can be compared with it. It is desirable to match the radiation levels from the standard and the unknown as well as possible for maximum precision. It is also desirable to match their shock impedances so that the reflected shock or release wave from the unknown sample can be used to estimate the Grunwalden parameter after its Hugoniot has been measured. An example of this type of experiment is shown in Fig. 9. Extremely accurate shock velocities can be obtained with this technique.



Fig. 9. Radiation from a quartz sandwich experiment done on a 2024 base plate. The radiation begins when the shock enters the first fused quartz plate and decreases when it enters the crystal plate and rises again when it enters the fused quartz cover plate. Relative intensities as well as shock velocities are measured.

If the radiation from the two materials are considerably different, filters can be used at one interface to match the radiation, but the shock velocity measurements will suffer accordingly as will the inherent precision in determining pressures in the three shock states from the radiation levels.

To abstract the temperature from these measurements one must calculate a radiation-temperature curve similar to Davis's, using the spectral response of the system over the appropriate frequency range.

The temperature of the standard for the experiment must be used to establish the relative intensity level for each measurement.

These experiments can be done using blocking filters so that windows with the greatest sensitivity can be employed. Time resolved spectral measurements can also be made. They can not be performed decently on multichannel devices that use a time integrated signal. However, we should make some spectral measurements so that the black body assumption can be checked, and to see if there are any regions of high spectral emission on absorption. To this end we are assembling a time resolved spectrometer to sample about ten spectral bands and a nontime resolved spectrometer to sample at 512 wave lengths.

#### RADIATION MEASUREMENTS FOR DETERMINING OVERTAKE VELOCITIES IN SYMMETRICAL IMPACTS

The rarefaction waves to be measured were generated with the widely used method of impacting a relatively thin driver plate onto a target plate. A drawing of the idealized shock-rarefaction process is shown in Fig. 10. This figure and others have been taken from a

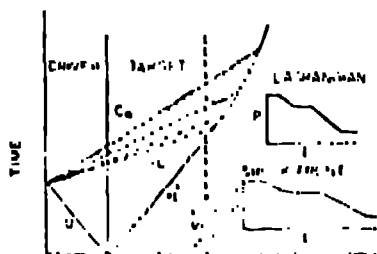


Fig. 10. Schematic of a shock and rarefaction from a symmetrical impact of an ideal elastic-plastic solid.

The bulk rarefaction wave further decreases the shock velocity to that governed by the tail characteristic. This state is determined by the pressure build up when the HE gases impinge on the back side of the driver when it is decelerated by the initial shock. We have indicated by the small inset drawing the basic difference between the type of experiments described here and those done with an insitu gauge or those that monitor velocities at an interface. If pressure and time were measured both gauges would record the same pressure levels of the different interactions. However, the time scales would not be the same and a linear transformation would not suffice to make them the same. In all the experiments described here we are monitoring the radiation emitted from the shock front.

If we restrict our attention to the lead characteristic it can be seen that by equating the time for the shock to go through the driver plus the time when the rarefaction through the driver and target catches the shock in the driver with that shock transit time then the Lagrangian sound velocity,  $c^L$ , is given by the following equation:

$$c^L = u_3(H+1)/(H-1) \quad (1)$$

Here  $U_s$  is the shock velocity and  $R$  the ratio of target to driver thickness where the catch up occurs. The sound velocity,  $C$ , in the shocked material is given by:

$$C = C^L (\rho_0/\rho) \quad (2)$$

where  $\rho_0/\rho$  is the ratio of the initial and final density. In this case the sound speed would correspond to the longitudinal component which we designate as  $C_L$ . The velocity of the second lead characteristic is referred to as the bulk velocity,  $C_B$ . Thus if  $R$  can be measured, the sound velocities can be determined.

In the preceding sections it was shown that from some transparent materials copious radiation is emitted from the shock front and that the amount is sensitive to pressure. Thus if we made the target thinner, so that the rarefaction wave has not yet overtaken the shock, and placed a piece of fused quartz on its front surface and observed the radiation emitted we might expect to see records like that in the lower insert (Fig. 10). It would be distorted in the  $P$  direction since we would be measuring relative light intensity, not pressure. Clearly we should be able to determine the time when the radiation begins to decrease, but also it is obvious that unless one knows almost everything about quartz that the sound velocity in the other material can not be determined. However, if several measurements were made on the same experiment at various target plate thicknesses the times,  $\Delta t$ , for the shock to be overtaken in the transparent material can be used to determine when the rarefaction would have overtaken the shock in the target. Since in this regime all the characteristics are linear it is obvious that these  $\Delta t$ 's are a linear function of the target thickness and when extrapolated to zero determines the position where the rarefaction wave would have overtaken the shock in the target. This position is independent of the properties of the transparent material, hence referred to as the analyzer. In Fig. 11 we have drawn the  $X-t$  solution for an impact experiment with the location and subsequent

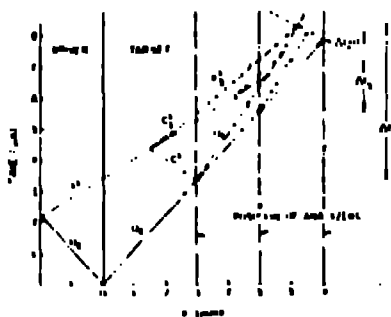


Fig. 11.  $x-t$  plot showing how by measuring the time for the rarefaction to overtake the shock in the analyzer that its velocity in the target can be determined.

interactions of three analyzers. In this figure the left going characteristic from the target-analyzer interaction have been drawn with the same slope, a case that exists if the analyzer has the higher shock impedance. This of course is immaterial if only the leading wave is considered.

In all the experiments the radiation is viewed through small (typically 1 mm diam) apertures placed as close as possible to the analyzers by light pipes ~15 mm away. Thus the signals are averaged over an area ~2 mm in diameter. Two baffles between the light pipes and apertures prevent most of the unwanted radiation in the system from entering the

light pipes. For explosive systems the target assembly is much like that shown in Fig. 12. Here five levels are indicated but sometimes ten or more have been used. The lower part of the assembly is used

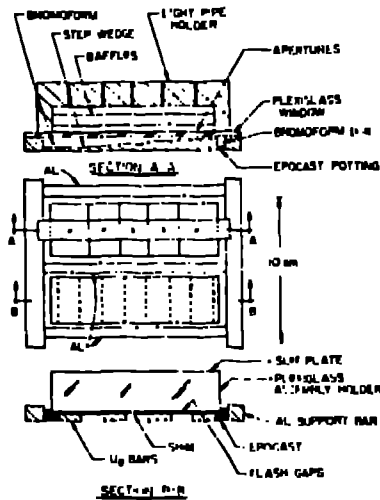


Fig. 12. Target assembly for high explosive experiments.

to measure the differential shock driver velocity,  $U_B$ , and hence establishes shock strength. These records also give a measure of bow and tilt so these effects on shock rise times can be accounted for. An assembly used for two stage gun experiments is shown in Fig. 13. In this particular assembly the steps are placed on a circular array on the impact side of the target. This keeps light coming from strong interactions at corners from complicating the records. Differential velocity measurements can also be made with this assembly by taking PM signals from thick and thin areas of the target and feeding them into the same oscilloscope with one set inverted. The rise and fall represent shock arrivals at the target analyzer interface and when coupled with the measured projectile velocity determine a Hugoniot point. A reproduction of a photographic record used to determine the shock pressure is reproduced in Fig. 14 and the type of oscilloscope record to measure shock velocities on the two stage gun in Fig. 15. From Fig. 14 it is found that the average time smear caused by bow and tilt over a two mm diameter area is about one ns in the region used to determine the overtake velocities. Records obtained in the central region have essentially no loss of time resolution due to tilt.

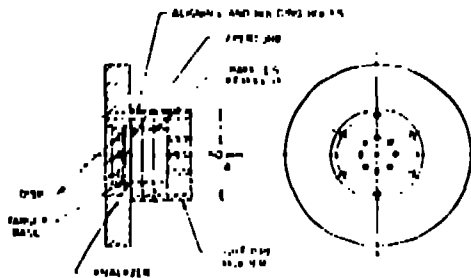


Fig. 13. Target Assembly for two stage gun experiments. Small disk on the impact side give the desired variable target thicknesses.

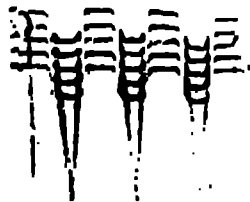


Fig. 14. A reproduction of a photographic record to determine the differential ( $U_S - U_D$ ) velocity and hence pressure.

We have used three materials as analyzers: fused quartz; a high density glass,  $\rho \sim 5 \text{ gm/cm}^3$ ; and bromoform,  $\text{Br}_3\text{HC}$ ,  $\rho \sim 3 \text{ gm/cm}^3$ . To demonstrate that the detection of the first overtake is independent of the analyzer, experiments were performed using all three on the same shot. Reproductions of the records are shown in Fig. 16 and the derived  $\Delta t$  vs thickness data in Fig. 17. The results of an experiment on 2024 Al designed to measure the first wave

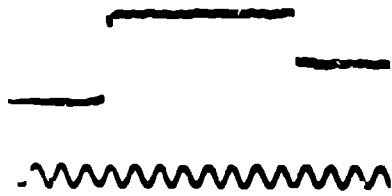


Fig. 15. An oscilloscope record showing how the differential velocity can be measured on the two stage gun.

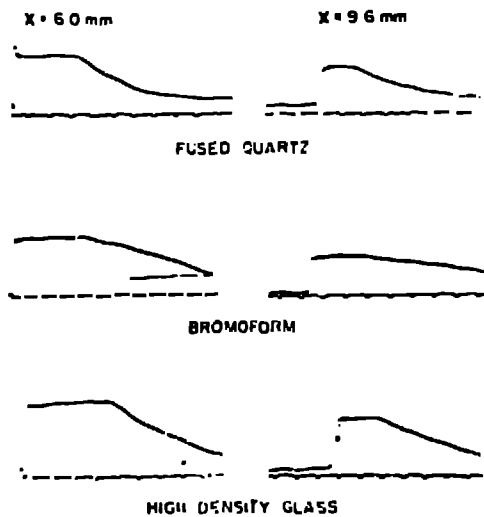


Fig. 16. Overtaking waves at two thickness seen by three different analyzers. The time marks are 0.1 us.

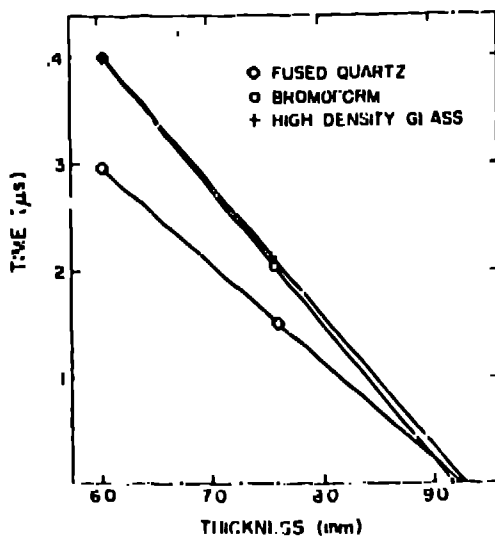


Fig. 17. The measured overtake time vs target thickness from the records of Fig. 16.

arrival are plotted in Fig. 18. The sigma for the catch up position determined from least square analysis of the data was 0.3%. Since the catch up ratio is approximately four for most materials these errors are reduced by approximately one half for the derived sound velocities.

Since the sound velocity is proportional to the shock velocity any errors in determining the shock strength are reflected directly in the derived sound speeds. However, this is really only very important if some phenomenon is occurring, such as a phase change where it is desirable to know the absolute value of the pressure. This is because these errors move the sound velocity along a curve that is nearly parallel to the true one. There is a source of error in the explosive experiments that is nontrivial. This is the change in driver plate thickness due to plate stretching while being accelerated. This is not a constant and varies from one explosive driver system to another. We have framing camera records that show that this can be as large as one percent in some geometries. Thin plate accelerated for short distances appear to have very little stretching. For example work done by Brown and McQueen<sup>9</sup> on iron show that explosive experiments done with thin drivers gave the same results as those performed on the two stage gun, which are not bothered by this effect.

So far we have restricted ourselves to measuring the lead characteristic. There is more information on the records but considerably less well defined and a lot less straight forward. A set of records (Fig. 19) for 2024-A1 gives an indication of what can be seen in regards to the elastic-plastic behavior of this material under strong shock conditions. In the three records on the left the first break in the traces is due to the longitudinal component of the release wave. The

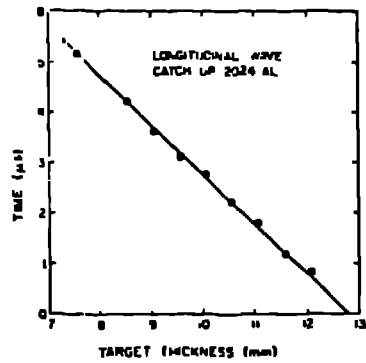


Fig. 18. The results from a very high quality set of records for determining overtake locations.

OVERTAKING WAVES IN 2024 AL AT 71 GPa

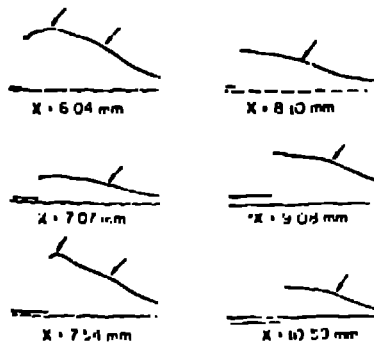


Fig. 19. Records showing the change in slope caused by the arrival of the bulk sound wave.

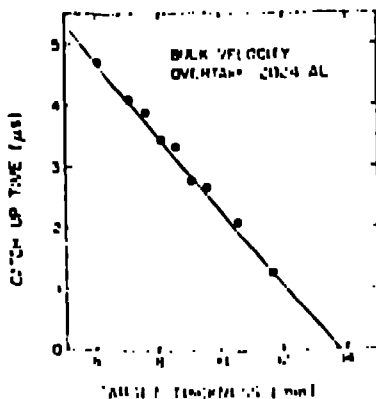


Fig. 20. Catch up time in the analyzer from records of Fig. 19.

second break much less well defined is due to the bulk velocity release. In the records on the right the longitudinal component has overtaken the shock wave in the target before reaching the analyzer and only the break from the bulk is present. The times for these breaks have been measured and are plotted in Fig. 20. In this set of records the second break was reasonably well defined. This is not always the case. The intercept gives an approximate value for the bulk sound velocity using the previous analysis. However, for an accurate value, the interaction of the analyzer (bromoform was used here) with the target must be accounted for as well as the shock degradation in the target due to the finite yield strength exhibited in the records. From the records it can be seen that the shock wave has traveled ~ 8 mm before being degraded by the longitudinal wave. The decrease in shock velocity for the remaining 5.5 mm of run can be accounted for in a reasonable manner. Another correction is needed to account for the decrease in pressure due to the longitudinal release. The bulk release velocity is actually centered on a somewhat lower pressure than that measured for the initial shock wave. A first order correction for this can be readily made. From our many measurements using bromoform as an analyzer we have determined the relative radiation intensity as a function of pressure in the 2024 Al target. Hence the pressure in the target can be estimated by the decrease in intensity of the bromoform. The equation for this is

$$P = P_0 - 47 \log (I_0/I) \quad (3)$$

where P is the pressure in GPa's and  $I_0/I$  the ratio of intensities. From the records it appears that there is about 10 GPa pressure release before the bulk wave is seen. Even though this looks like a large correction the fact that the R values change very little with pressure implies that even considerable errors in making this correction will have but a small effect on the bulk sound velocity vs

pressure locus. This measurement can be used to estimate the yield strength but there will be fairly large errors since this is a differential measurement. It should be noted that the records on the right have one less perturbation, that caused by the interaction of the longitudinal release wave with the analyzer, which makes the system somewhat less complicated. Using bromoform for an analyzer also has the advantage that its behavior should be ideally perfectly plastic.

The Grüneisen ratio,  $\gamma_g$  can be obtained from these measurements from the following equation<sup>9</sup>

$$\gamma = \frac{[(dP/dV)_{HUG} - (dP/dV)_S]2V}{P_H + (dP/dV)_{HUG} (V_0 - V_H)} \quad (4)$$

where the standard notation has been used and

$$(dP/dV)_S = -(\rho C_B)^2 \quad (5)$$

Bulk sound velocities calculated so far are in good agreement with those calculated with  $\rho\gamma = \text{constant}$ .

Work in progress on Cu and 2024 Al indicates that melting does not begin to occur until around 190 GPa in 2024 Al and 160 GPa in Cu. Calculations<sup>10</sup> done earlier indicated that the Cu Hugoniot would cross the melting phase line at about 133 GPa. A tentative explanation for this discrepancy is that the electronic contribution to the specific heat was not used in those calculations. This would have very little effect on the calculated phase line since it was neglected for both phases. However, it would cause the calculated temperatures along the Hugoniot to be too high causing the Hugoniot to cross the phase line at too low a pressure. More data are needed to determine these points more precisely and also the pressures where the materials appear to be completely melted.

#### OVERTAKING VELOCITIES IN UNSYMMETRICAL IMPACTS

It is unfortunate that symmetrical impacts cannot be used with all the materials that one would like to investigate. This is especially true with the explosive experiments where it is just not possible to accelerate some materials to the velocities desired without breaking them. If the driver has been well characterized it is possible to use it to impact other materials to determine these rarefaction wave velocities. Again if we equate the appropriate times for the catch-up equation but distinguish the driver and target with the appropriate subscripts (D and T) we obtain the following:

$$\frac{R}{U_T} = \frac{1}{U_0} + \frac{1}{C_D} + \frac{R}{C_T} \quad (6)$$

so

$$\frac{1}{C_T} = \frac{1}{U_T} - \frac{1}{R} \left( \frac{1}{U_0} + \frac{1}{C_D} \right) \quad (7)$$

but 
$$C^L = R^*U \quad (8)$$

where 
$$R^* = (R+1)/(R-1) \quad (9)$$

then 
$$\frac{1}{R^*T} = 1 - \frac{1}{R} \frac{U_T}{U_D} \left\{ 1 + \frac{1}{R^*} \right\} = 1 - F/R \quad (10)$$

and hence 
$$C_T = (U_S - U_P)_T R_T^* \quad (11)$$

As would be expected, C is more sensitive to errors in measuring R, which is the actual catch up ratio of the experiment, than in the symmetrical experiments.

The results of these measurements, as in the symmetric impact ones, are quite insensitive to errors made in determining pressure. Moreover they are reasonably insensitive to errors in the values of R used for the driver. In our work on 2024 Al it was found to be necessary to use iron drivers if we were to go completely through the melting region. Using  $R^*$  vs P determined from the data from Ref. 8 below the transition region, we find that the value of F in the above equations changed almost linearly from 2.29 at 80 GPa to 2.346 at 160 GPa. The other pressure dependent term,  $(U_S - U_P)_T$ , changes only ten percent in that pressure regime. It is felt that it will be almost impossible to extract any useful knowledge of the elastic-plastic behavior if a material like iron is used for the driver. The bulk velocities will also be difficult, if not impossible, to measure accurately. Since there are some materials, minerals for example, for which it would be desirable to know both the longitudinal and bulk wave velocities, we are planning to characterize a lead alloy, so that elastic-plastic behavior caused by the driver will not be present. This material can then be used as impactors on the gun experiment.

It is probably obvious, but in all these experiments the driver should impact the material of interest directly without any intervening base plate.

If the material to be investigated is transparent it can be used as its own analyzer. By using the equation of state of the driver and target materials to determine the shock velocity in the target and by measuring the time when the radiation begins to decrease, the catch up ratio can be calculated. If the target is made of several layers which have had a thin film of aluminum deposited on them, so that light transmission is reduced by ten percent or so, then it should be possible to measure the shock velocity in the target directly. Fig. 21 illustrates this. Oscilloscope traces are reproduced in Fig. 22 to illustrate the type of measurements that can be made. These are all bonded layers of fused quartz impacted by an iron driver. Epoxy is used to bond the layers together because its setting time is long. Pieces are thoroughly cleaned and put in a press with a small drop of epoxy in each layer. A plastic cushion is used to maintain pressure and to avoid breaking samples. In the

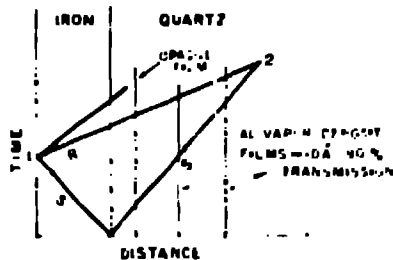


Fig. 21. Schematic for measuring overtake and shock velocities in transparent targets. The opaque film shields unwanted light.

record on the left small discontinuities in the trace can be seen. In the originals these are seen to be small decreases in the radiation caused by glue on the interfaces. This was because insufficient pressure was used in the assembly. The other records show no indication of this, but do show a finite rise time as the shock front passes through the interfaces. It is felt that the increase in radiation is indeed an almost real replica of the shock front. That is, these windows are in a sense acting like insitu gauges. The slow rise time (ten ns is typical) observed is probably real. This could be due to the fact that

quartz has a very large phase change and this must be done in the shock front. These records as well as the others are read with an optical comparator that digitizes the record. These are put in the comparator, which displays the records on a screen. Selected areas, for example two adjacent interfaces, are magnified and normalized in amplitude. They can then be matched and the time between them measured. Thus the whole trace in the region of interest is used to obtain velocity measurements.



Fig. 22. Records showing shock wave arrivals in fused quartz.

It occurred to us that if we could introduce a small perturbation in the target causing a small short pressure pulse, it might just be possible to see it reflected back from the driver-target interface. If this could be measured the sound velocity could be measured independent of the driver properties. There was also the possibility that this perturbation might travel at bulk sound velocity if the target was on its upper yield surface. Quite thick shims were used in the first experiments so that we could be sure to see something. It didn't take much to put huge perturbations on the records. Later records using thinner shims are reproduced in Fig. 23. The perturbation of interest in the records generally has a decrease followed by a rise. The last record on the right is what was expected. The small decrease probably were caused by glue joints. The perturbations should be deposited rather than glued in place. The smallest aluminum shim stock available here, seven microns produced the small pulse seen in the third figure. If



Fig. 23. Four records showing the reflection from a small perturbation in the target reflecting back from the higher impedance driver and eventually overtakes the shock wave.

a represents the distance of the perturbation from the impact interface and b the distance from it when it overtakes the shock, then the Lagrangian velocity is given by

$$c^L = U_s(2a + b)/b \quad (12)$$

These experiments can be done with the overtake experiments just described.

#### SUMMARY

Several applications utilizing the radiation from shocked transparent materials have been described. These include making temperature measurements on transparent materials, determining the longitudinal sound velocity at pressure and for some materials the bulk velocity, which then can be used to calculate the Grüneisen parameter and the shear modulus at pressure. Estimates of the yield strength can also be made. These experiments have led to techniques for making very accurate shock velocity measurements.

#### ACKNOWLEDGMENTS

This work was performed under the auspices of the United States Department of Energy.

#### REFERENCES

1. J. M. Walsh and R. H. Christian, *Phys. Rev.* **97**, 1544 (1955).
2. S. B. Kormer, M. V. Sinitayn, G. A. Kirillov and V. O. Urtin, *Sov. Phys. JETP* **21**, 689 (1965).
3. L. V. Al'shuler, M. I. Brazhnik, and G. I. S. Telegin, *J. Appl. Mech. Tech. Phys.* **12**, 971-976, (1971).
4. J. N. Fritz and J. A. Moran, *Rev. Sci. Instrum.* **44**, ? (1973).
5. L. M. Barker, IUTAM Symposium, Paris, 1967, Gordon and Breach.
6. G. A. Lyzenga and T. J. Ahrens, *Geophys. Res. Lett.* **7**, 141, (1980).
7. J. M. Walsh, M. H. Rice, R. G. McQueen, and F. L. Yarger, *Phys. Rev.* **103**, 196 (1957).
8. J. M. Brown and R. G. McQueen, *Geophys. Res. Lett.* **7**, 533, (1980).
9. R. G. McQueen, *Metall. Soc. Conf. Vol. 22*, Gordon and Breach, NY 1964.
10. R. G. McQueen, W. J. Carter, J. N. Fritz and S. P. Marsh, NBS Spec. Publ. 376, E. C. Boyd ed. (1968).